



The fatty acid elongase gene family in the brown planthopper, *Nilaparvata lugens*



Dan-Ting Li^a, Xuan Chen^a, Xin-Qiu Wang^a, Bernard Moussian^b, Chuan-Xi Zhang^{a,*}

^a State Key Laboratory of Rice Biology, Ministry of Agriculture Key Lab of Molecular Biology of Crop Pathogens and Insects, Institute of Insect Science, Zhejiang University, Hangzhou, 310058, China

^b Université Côte d'Azur, CNRS, Inserm, Institute of Biology Valrose, Parc Valrose, 06108, Nice Cedex 2, France

ARTICLE INFO

Keywords:

Nilaparvata lugens
Fatty acid elongase
RNA interference
Lipid metabolism
Cuticular hydrocarbon
Waterproofing

ABSTRACT

The cuticular hydrocarbon (CHC) biosynthetic pathways branches off from the synthesis of fatty acids. Fatty acid elongases (ELOs) are enzymes catalyzing the synthesis of long-chain fatty acids and thereby contribute to the diversification of CHCs. Based on bioinformatics analyses we identified 20 ELO genes in the brown planthopper, *Nilaparvata lugens*. RNA interference against these genes demonstrated that 9 *NIELO* genes were essential for the survival of *N. lugens* nymphs and adults. Indeed, knockdown of *NIELOs* 1, 3, 4, 7, 8, 9, 10, 12 and 18 caused lethal phenotypes with a thin and wizened body and reduced lipids in the fat body. Surface analysis by scanning electron microscopy and CHC quantification indicated that knockdown of *NIELOs* 2, 3, 8 and 16 additionally resulted in a smooth body surface and a decrease in CHC amounts. Therefore, we speculate that long-chain CHCs are needed for CHC attachment to the cuticle surface. CHC deficiency, in turn, resulted in increased adhesion of water droplets and secreted honeydew to the animal surface and the inability of *N. lugens* to survive in paddy fields with varying humidity. Our present study provides an initial comprehensive analysis of ELO gene functions in an insect, and may serve to better understand the biology of CHCs.

1. Introduction

Fatty acid elongases (ELO), which are widely expressed in various organisms, including animals, plants and microorganisms, play crucial roles in regulating the length of fatty acids and therefore their functions and metabolic fates (Guillou et al., 2010). Fatty acids elongation is achieved with four separate enzymatic reactions: condensation, reduction, dehydration and another reduction. ELO catalyzes the initial and rate-controlling condensation reaction (Denic and Weissman, 2007; Guillou et al., 2010). In insects, ELOs contribute to various biological processes, such as mating, fecundity, pheromone biosynthesis and cuticle functions (Chertemps et al., 2007; Leonard et al., 2004). The numbers of ELOs differ among insect species. There are 20 ELOs in *Drosophila melanogaster*, 19 in *Plutella xylostella*, 18 in *Tribolium castaneum*, 17 in *Anopheles gambiae*, 15 in *Danaus plexippus*, 14 in *Apis mellifera*, 13 in *Bombyx mori*, and 12 in *Acyrtosiphon pisum* (Zuo et al., 2018). All ELO proteins contain a characteristic ELO domain (pfam PF01151) and a highly conserved HXXHH motif, which is conserved in the yeast, mouse, rat and human ELO proteins (Jakobsson et al., 2006; Tvrdik et al., 2000). Unlike mammals, the number of functionally verified ELO genes in insects is quite limited. *Elo68a*, the first identified

insect elongase gene in *Drosophila melanogaster*, was shown to elongate myristoleic and palmitoleic acids in adult males (Chertemps et al., 2005). Thereafter, the *Elo68β*, *EloF*, *bond*, *sit* and *noa* genes were identified by homology searches based on the *D. melanogaster* genome database. *EloF*, which is a female-biased expressed ELO in *D. melanogaster*, is essential for the biosynthesis of long-chain hydrocarbons and courtship behavior (Chertemps et al., 2007). *Bond*, catalyzing the production of very long-chain fatty acids, is involved in the male sex pheromone CH503 synthesis and plays important roles in male fertility (Ng et al., 2015; Szafer-Glusman et al., 2008). The elongase coded by *noa* (also known as *baldspot*) is most similar to the mammalian elongase ELOVL6, and is needed for viability (Jung et al., 2007). In other insect species, two ELO genes (*TmELO1* and *TmELO2*) from the yellow mealworm (*Tenebrio molitor* L.) involved in long chain and very long chain fatty acids synthesis were also identified and characterized (Zheng et al., 2017). The expression patterns of some ELO genes, which may be associated with the biosynthesis of CHCs, were systematically analyzed in the honeybee *Apis mellifera* (Falcon et al., 2014). ELO genes from *Bombyx mori*, *Tribolium castaneum*, *Anopheles gambiae* and *Acyrtosiphon pisum* had been systematically identified and analyzed based on genomic and transcriptomic databases, but their functions remain

* Corresponding author.

E-mail address: chxzhang@zju.edu.cn (C.-X. Zhang).

<https://doi.org/10.1016/j.ibmb.2019.03.005>

Received 31 January 2019; Received in revised form 8 March 2019; Accepted 12 March 2019

Available online 16 March 2019

0965-1748/© 2019 Elsevier Ltd. All rights reserved.

unclear.

The brown planthopper, *Nilaparvata lugens* Stål (Hemiptera: Delphacidae), is a typical rice monophagous insect that feeds only on phloem sap of the rice plant and excretes honeydew (Xue et al., 2014). This insect is the number one rice pest in many Asian countries, causing a serious yield loss of rice every year (Bottrell and Schoenly, 2012). A complex behavior with winged 'macropterous' and truncate-winged 'brachypterous' forms, the ability of long distance migration, a great power in reproduction and the competence in strong adaptation to variable environments together render *N. lugens* a pest, which is very difficult to control (Huang et al., 2017). *N. lugens* has been extensively studied as a model in ecological systems and recently as a representative hemimetabolous insect in molecular biology. However, fatty acid elongation has rarely been studied in hemimetabolous insects. As oxidative decarbonylation in the last step of hydrocarbon biosynthesis has little chain-length specificity, it is considered that ELO activities are performed by many ELOs, which have chain-length specificity (MacLean et al., 2018; Qiu et al., 2012; Tillman et al., 1999; Tillmanwall et al., 1992). Chain lengths of insect CHCs (21–50 carbons) provide a hydrophobic coating against water loss at the body surface (Chung and Carroll, 2015; Gibbs, 1998). Using chemical or genetic methods to remove the outermost hydrophobic layer can render insects particularly sensitive to desiccation (Billeter et al., 2009; Wigglesworth, 1945). As *N. lugens* survive in paddy fields with different humidity levels, we are interested in the composition of their outermost layer, which is built to control water balance. In particular, we are interested in the key genes involved in biosynthesis of cuticular lipids that adhere to the hydrophobic cuticle surface, the envelope (Locke, 2001). In this study, we screened 20 ELO genes of *N. lugens* (NIELOs) that we identified based on their homology to *D. melanogaster* and other insect elongases. The gene architecture, phylogenetic relationship, expression profiles and RNA interference (RNAi) effects of NIELOs were analyzed to reveal their biological functions in the context of *N. lugens* growth, development and life style. In particular, we analyzed the integument surface ultrastructure of dsRNA-treated *N. lugens* by scanning electron microscopy (SEM), and analyzed their CHCs by quantitative GC-MS approaches to investigate the ELO gene function in the CHC pathway and possible roles in insect cuticle waterproofing and water retention.

2. Materials and methods

2.1. Insects

N. lugens used in this study were originally obtained from rice fields in Hangzhou (30°16'N, 120°11'E), China. They were maintained on rice variety Xiushui 134 in a greenhouse of Zhejiang University at 26 ± 1 °C and 60 ± 5% relative humidity under a photoperiod of 16:8 h (light:dark).

2.2. Identification and analysis of ELO coding sequences

Base on a bioinformatics analysis, genes encoding ELO proteins were screened from the *N. lugens* genomic (GenBank accession numbers: AOSB00000000) (Xue et al., 2014) and transcriptomic databases by using the amino acid sequences of the ELO genes from *D. melanogaster*, *B. mori* and *A. mellifera*, which were obtained from FlyBase (<http://flybase.org/>), SilkDB (<http://silkworm.genomics.org.cn/>) and NCBI, respectively (Table S1). The ELO cDNA sequences were obtained from the local transcriptomic databases, and the predicted ORFs were confirmed by RT-PCR. Primers used in RT-PCR are shown in Table S2.

2.3. Phylogenetic tree construction for ELO genes

The amino acid sequences of ELO genes were deduced from the corresponding cDNA sequence using the translation tool on the ExpASY SIB Bioinformatics Resource Portal (<http://web.expasy.org/translate/>).

Amino acid sequence alignments were carried out with ClustalX and GeneDoc. To construct a phylogenetic tree among the amino acid sequences of ELO proteins, the maximum likelihood algorithm analysis with the JTT model for amino acids and 1000 bootstrap replicates and all branches with a value less than 50% collapsed was implemented in MEGA 7. The sequences that have been identified from *Homo sapiens*, *Mus musculus*, *Canis lupus familiaris*, *Gallus gallus*, *B. mori*, *D. melanogaster*, *Danaus plexippus*, *Plutella xylostella*, *T. castaneum*, *A. pisum*, *A. mellifera*, *A. gambiae*, *Arabidopsis thaliana*, and *Saccharomyces cerevisiae* (GenBank accession numbers are provided in Table S1) were used in this analysis.

2.4. Total RNA isolation and first-strand cDNA synthesis

Total RNAs of various developmental *N. lugens* or different dissected tissues were isolated by using a TRIzol Total RNA Isolation Kit (Takara, Kyoto, Japan). Developmental samples of nymphs (fourth- and fifth-instar) and adults (male and female) were collected every twenty-four hours after molting. Tissue samples (integument, fat body, gut, ovary and testis) were dissected from adult *N. lugens*. First-strand cDNA was synthesized using HiScript® II Q RT SuperMix for qPCR with gDNA wiper Mix (Vazyme Biotech Co., Ltd., Nanjing, China) following the manufacturer's protocol.

2.5. Real-time qPCR analyses

To investigate the expression profiles of NIELOs, real-time qPCR (RT-qPCR) was conducted using a Bio-Rad real-time PCR system (BioRad, Hercules, CA, USA), and a 20 µl reaction contained 2 µl of 10-fold diluted cDNA, 0.6 µl of each primer and 10 µl ChamQ SYBR Color qPCR Master Mix (Vazyme Biotech Co., Ltd., Nanjing, China). The *N. lugens* housekeeping gene, 18 S ribosomal RNA (*NI18S*: JN662398.1), was used as an internal control. Gene-specific primers are listed in Table S2. The qPCR program was operated: 95 °C for 30 s followed by 40 cycles at 95 °C for 5 s and 60 °C for 30 s. Quantitative variations were evaluated by using a relative quantitative method ($2^{-\Delta\Delta Ct}$) and normalized with *NI18S* expression (Livak and Schmittgen, 2001). Each treatment was conducted in three independent biological replicates with three technical replicates.

2.6. RNAi effects on *N. lugens*

dsRNAs was synthesized by using a MEGAscript T7 Transcription kit (Ambion, Austin, TX) from the purified DNA templates. Two unique regions of each *N. lugens* ELO gene were designed to synthesize dsRNAs. The primers used are listed in Table S2 dsGFP was used as a negative control. dsRNA microinjection against *N. lugens* was carried out according to a previously reported method (Pan et al., 2018; Xu et al., 2015). One hundred second- (day 2), fourth-instar (day 1) nymphs, male fifth-instar (day 1) nymphs or newly emerged adults were used for microinjection treatment. Each treatment was conducted in three biological replicates. In all, ~5, 10, 15, 20 nl of dsRNA (5 µg/µl) was injected into each second-, fourth- and fifth-instar nymphs and adults, respectively. Samples contained six to eight insects were collected to evaluate the RNAi efficiency of NIELOs three days after injection by RT-qPCR. Other insects were used for development observations and survival quantification.

One pair, a treated male & a healthy female or a healthy male & a treated female, 2 days after injection, were transferred onto fresh rice seedlings in glass tube to produce offspring for 3 d. Subsequently, the insects were removed onto fresh rice seedlings in new glass tubes for calculating the lifespan, and the eggs/seedlings were maintained for 10 d for counting the number of hatched offspring. The leaves and stems of the rice seedlings were dissected under the microscope to count the number of eggs failing to hatch. Each target gene was carried out for 10 biological replicates.

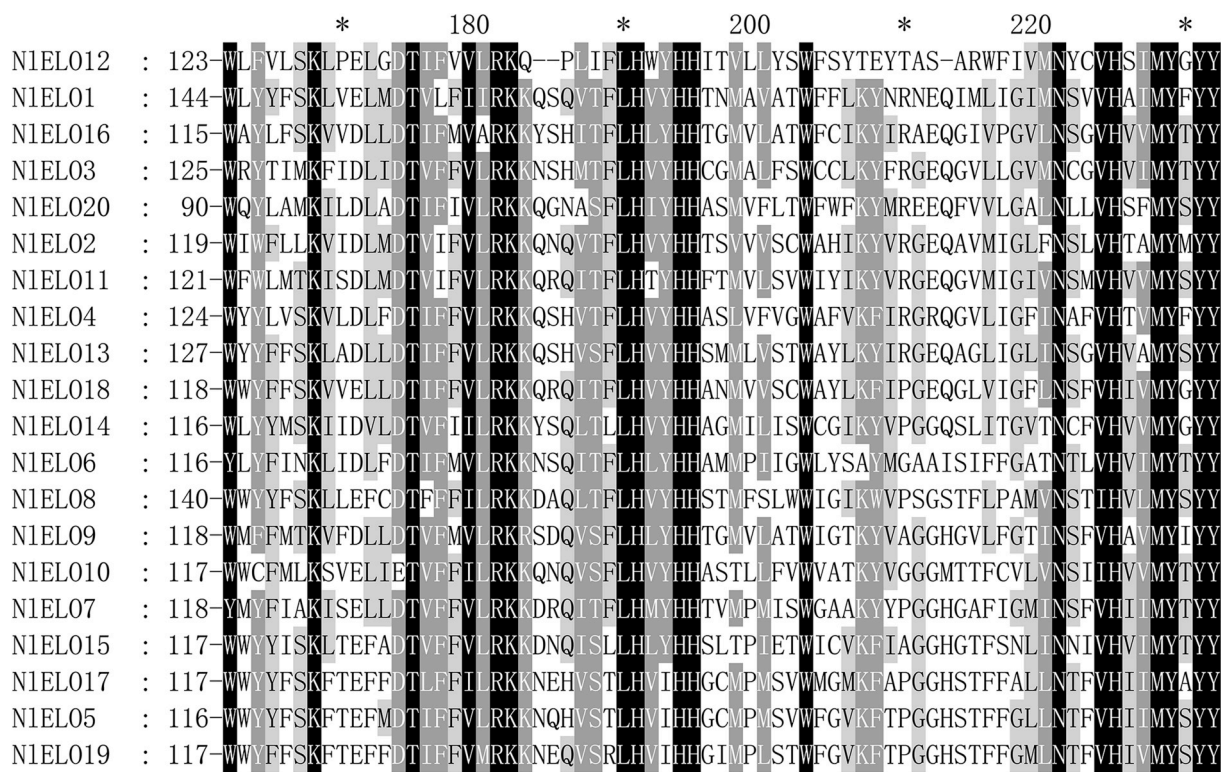


Fig. 1. Sequence alignment of *N. lugens* ELO proteins. Identical amino acid residues and conservative substitutions are shaded in black and gray, respectively. The conserved histidine motif HXXHH (double underline) and the conserved motif YXXX (black line) are indicated.

2.7. Examination of body weight and triglyceride content in dsRNA-treated *N. lugens*

One hundred fourth-instar (day 1) nymphs were used for ds*NIELOs* 7, 9, 10, 12 and ds*GFP* injection. Five fifth-instar (day 3) nymphs, female adults and male adults (3 days after eclosion) were collected for body weight examination. Each treatment was conducted in sextuplicate. For triglyceride content analysis, three fifth-instar (24 h after ecdysis) nymphs were collected for measurement according to the manufacturer's instructions.

2.8. Waterproofing and water retention assay

Two hundred fourth-instar (day 1) nymphs were used for ds*NIELOs* 2, 3, 8, 16 and ds*GFP* injection. After three days, thirty newly injected fifth-instar nymphs were collected and released into test plastic containers that were filled with sufficient fresh rice plants. Then, 5 cm³ of water was sprayed straight down into the container every 12 h by a mini-sprayer. After each addition of water, the number of surviving *N. lugens* in every treatment group was recorded. Each experiment was conducted in triplicate. All test containers were placed in an artificial cabinet at 26 ± 1 °C, with 60 ± 5% relative humidity under a photoperiod of 16:8 h (light:dark).

For the desiccation tolerance bioassay, fifth-instar (day 3) nymphs were injected with ds*NIELOs* 2, 3, 8, 16 and ds*GFP*. Thirty nymphs were subjected to desiccation treatment (< 5% RH) at 26 ± 1 °C for 9 h without food. The number of surviving nymphs was counted every half hour. In control experiments, nymphs were starved at the same temperature with a 60–70% RH.

2.9. Eosin Y staining and Nile-Red Staining

To analyze cuticle penetration, fifth-instar nymphs (48 h) were incubated with Eosin Y according to the method of Wang et al. (2016).

Nymphs were anaesthetized with CO₂ and transferred into a 1.5 ml micro-centrifuge tube containing 1 ml dye solution (0.5% Eosin Y (W/V) and 0.1% Triton X-100). After 30 min of staining at the 37 °C, nymphs were washed three times with tap water at 25 °C before microscopy.

For lipid staining, Nile-Red Staining was conducted according to the method of Lu et al. (2018). Fat bodies of fifth-instar nymphs (48 h) were dissected in the precooled PBS buffer (pH = 7.4) and the adherent tissues were carefully removed with forceps as thoroughly as possible under a stereomicroscope. The dissected fat bodies were fixed with 4% paraformaldehyde on a glass slide for 2 h at 25 °C and then washed with PBS for three times (3 × 5 min). Then, fat bodies were submerged in Nile red solution [1 µl of Nile red (1 mg/ml) in 100 µl of PBS] and visualized using a Zeiss LSM 800 confocal laser microscopy (Carl Zeiss MicroImaging, Göttingen, Germany) within 2 h.

2.10. Scanning electron microscope (SEM) observation

For SEM analysis, ds*NIELOs* 2, 3, 8, 16- and ds*GFP*-treated fifth-instar (48 h) nymphs were placed on a stub and dried in an ion sputter (Hitachi, Tokyo, Japan) under a vacuum. After gold sputtering, the samples were observed under SEM (TM-1000, Hitachi, Tokyo, Japan). To analyze cuticular lipids of *N. lugens*, the dsRNA-treated insects were directly observed under SEM according to the method of our previous study (Li et al., 2019). Each treatment was observed in triplicate.

2.11. Extraction and quantification of CHCs

CHCs of *N. lugens* were extracted from fifth- (day 3) instar nymphs after injection following a procedure of our previous study (Li et al., 2019). Briefly, 20 nymphs (approximately 15 mg each) were immersed in 200 µl *n*-hexane together with 500 ng *n*-heneicosane (C₂₁) as an internal standard. The solvent was stirred gently for 3 min and then drawn with a glass Pasteur pipette into a clean chromatography vial.

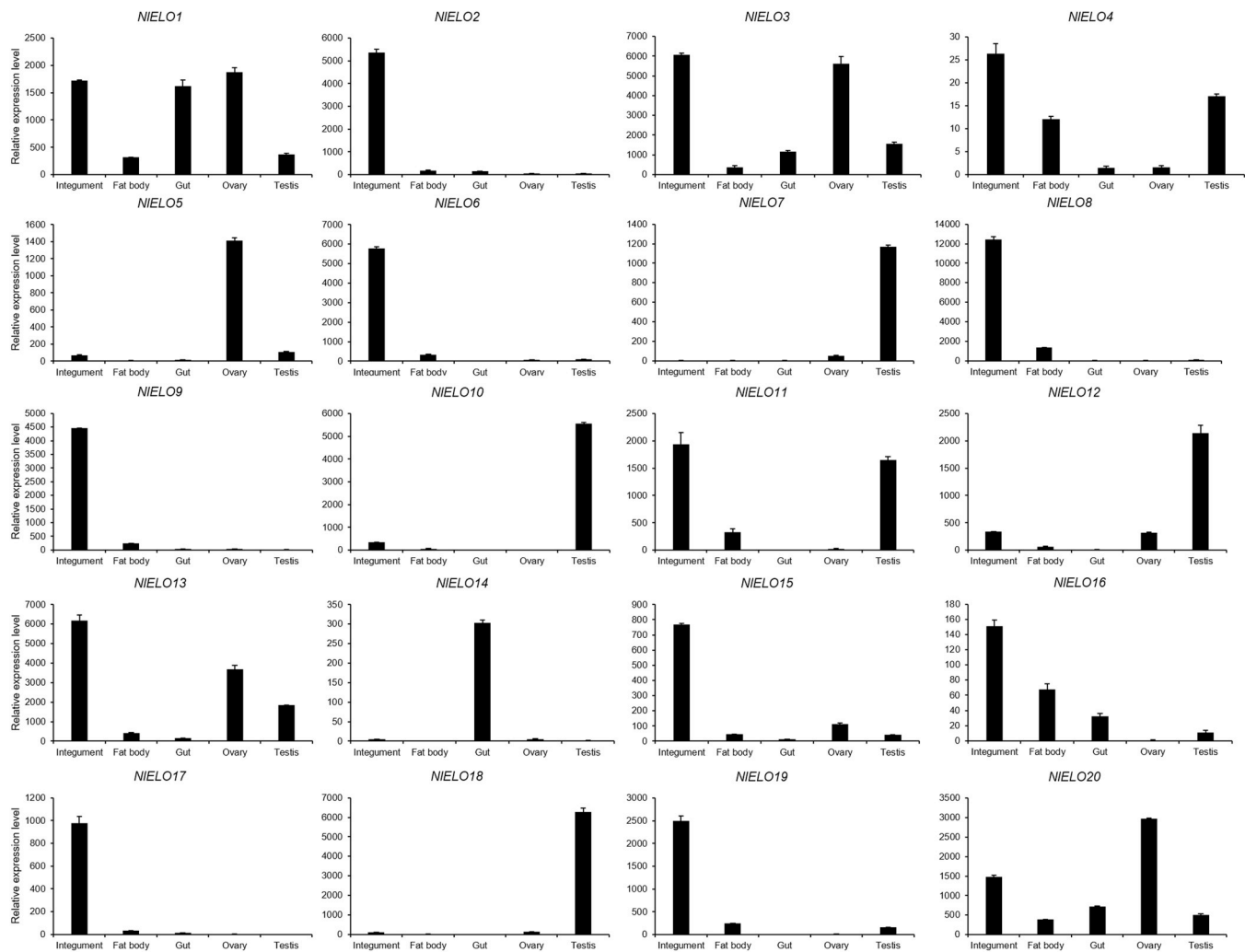


Fig. 2. Tissue-specific expression of ELO genes. Each total RNA was extracted from the integument, fat body, gut, ovary and testis of *N. lugens*, respectively. RT-qPCR and the $\Delta\Delta Ct$ method were used to measure the relative transcript levels of ELO genes in tissues. The relative expression levels of each ELO gene were normalized using *NIELO8* rRNA threshold cycle (Ct) values. The results of three biological replicates are shown with the standard deviations.

Repeated this procedure twice, and finally use 200 μ l hexane to rinse the nymphs and vial. Combined all the extracted hexane and dried to 200 μ l under high-purity nitrogen gas. Then the hexane extracts were loaded onto an \sim 300 mg silica gel (70e230 mesh, Sigma-Aldrich, Louis, MO, USA) mini-column in a glass wool-stoppered Pasteur pipette. The HC fraction was eluted with 2 ml hexane, taken to dry absolutely under nitrogen gas, and resuspended in 100 μ l hexane. The samples were analyzed on a TRACE 1310 (Thermo Scientific, Waltham, MA, USA) gas chromatograph (GC) was equipped with an ISQ single quadrupole MS and interfaced with Xcalibur 2.2 software. The constant flow of Helium was 1 ml/min. Splitless injection of 1.0 μ l was made into a 30 m \times 0.32 mm \times 0.25 μ m HP-5MS UI capillary column (Agilent Technologies, Santa Clara, CA, USA). The temperature program was operated: 60 $^{\circ}$ C for 2 min, then 5 $^{\circ}$ C/min to 320 $^{\circ}$ C, hold 10 min. The temperatures of injector and detector were set at 300 and 280 $^{\circ}$ C, respectively. Mass detection was run under an EI mode with a 70 eV ionization potential and an effective m/z range of 45–650 at a scan rate of 5 scan/s.

3. Results

3.1. Identification and analysis of ELO genes

We used the amino acid sequences of *D. melanogaster* and other

known insect ELO genes obtained from FlyBase and GenBank as queries to searches of the *N. lugens* genomic and transcriptomic databases. In total, twenty different genes encoding ELO were identified. The number of ELO proteins is the same in *N. lugens* and *D. melanogaster*. In the *N. lugens* ELO family, genes were named in the order in which they were phylogenetically analyzed. Each ELO gene was further confirmed by RT-PCR and sequencing, and deposited in GenBank (accession numbers MG573173–MG573192). Analyses of the predicted amino acid sequences in the NCBI Batch CD search indicated that the genes indeed encoded ELOs as they shared characteristic domains of eukaryotic ELOs, including a HXXHH motif and a YXYY motif in the domain (Fig. 1 and Fig. S1) (Chertemps et al., 2007).

Phylogenetic analysis was performed to investigate the evolutionary relationship of ELOs from *N. lugens* and other insect species, resulting in a bootstrap consensus tree (Fig. S2). This analysis suggested that the ELO genes were clustered into six groups (I–VI), four of which contained 7 *N. lugens* ELO genes: *NIELOs* 1–4 in group I, *NIELO5* in group III, *NIELO7* in group IV, and *NIELO20* in group VI. Six insect ELO genes from *A. gambiae*, *D. melanogaster*, *P. xylostella*, *B. mori*, *A. mellifera* and *T. castaneum* were clustered into group II, while no *N. lugens* ELO genes belonged to this group. Group V contained only *D. melanogaster* ELO genes, suggesting an ELO gene amplification event in this species. ELO gene duplication may also exist in *N. lugens*, as *NIELOs* 10 and 11 were in the one branch with no other insect ELOs. All of the ELO genes that

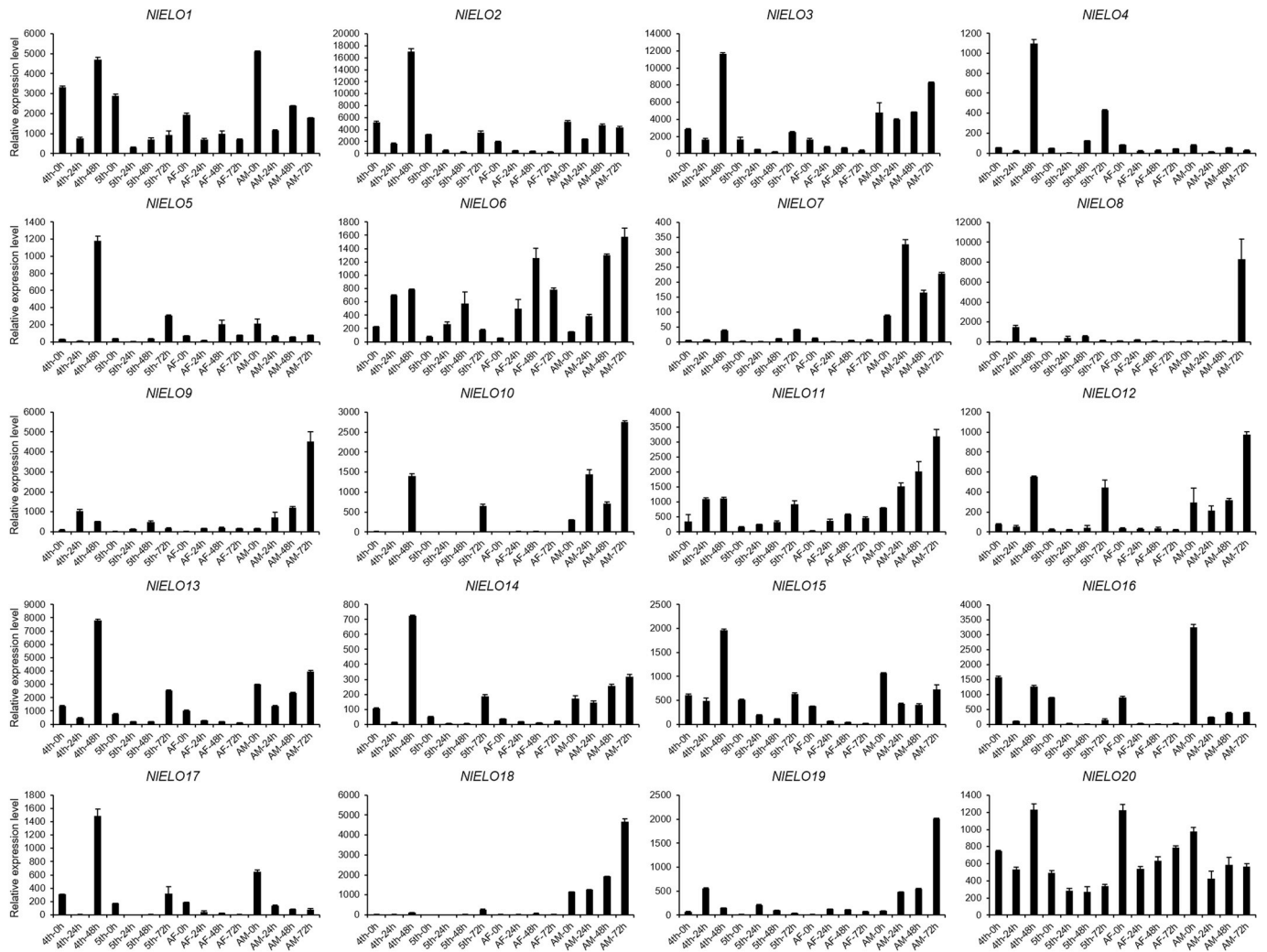


Fig. 3. Analysis of ELO genes during *N. lugens* development. Each total RNA samples were collected and extracted every 24 h from the beginning of each stage (n = 50 nymphs for fourth- and fifth-instars; n = 30 female adults and male adults). RT-qPCR and the $\Delta\Delta C_t$ method were used to analysis the relative expression levels of ELO genes. The relative expression levels of each ELO gene were normalized using *NI18S* rRNA threshold cycle (C_t) values. The results of three biological replicates are shown with the standard deviations.

could not be clustered in any group were highly divergent, indicating that more groups will be formed as more ELO genes are sequenced in different insect species in future.

3.2. Expression profile of NIELOs

The expression profiles of the *NIELOs* across the developmental stages and tissues were determined by RT-qPCR. A tissue-specific analysis of expression in adults showed that the *NIELOs* 2, 6, 8, 9, 15, 16, 17 and 19 transcripts were expressed at a notably high level in the integument and at low levels in the fat body, gut, ovary, and testis, indicating that these genes might play specific roles in the insect cuticle (Fig. 2). *NIELOs* 7, 10, 12 and 18 transcripts were notably high in the testis but low in the integument, the fat body, the gut and ovaries. *NIELOs* 5 and 14 were exclusively expressed in the ovary and the gut, respectively. Both *NIELOs* 3 and 13 were mainly expressed in the integument, ovaries and testes. Only *NIELO20* was mainly expressed in the ovary. *NIELO4* showed high transcript levels in the integument, the fat body and testes, while *NIELO1* was mainly expressed in the integument, the gut and ovaries.

During development, *NIELOs* 7, 10, 12 and 18, which were highly expressed in the testis, and *NIELOs* 8, 9 and 19, which were highly expressed in the integument, were male-biasedly or male-specifically expressed in adults, and their expression increased with time (Fig. 3). The transcripts of *NIELOs* 2, 3, 13, 14, 15 and 20 were at a notably high level in fourth-instar nymphs (48 h). *NIELOs* 4 and 5 exhibited similar expression patterns with transcript levels peaking periodically approximately 12 h before molting in fourth and fifth instar nymphs. Some new CHCs appeared on the newly molted insect are made prior to the molt, suggesting that *NIELOs* 4 and 5 might play important roles in the production of CHCs and the process of molting. *NIELOs* 1 and 16 were expressed in waves with periodical peaks in their transcript levels at the beginning of each developmental stage (0–2 h), suggesting that *NIELOs* 1 and 16 might have time-specific functions associated with the formation of new cuticle formation. *NIELOs* 6 and 17 showed very high transcript levels at late fourth instar and adult stages, respectively.

3.3. Phenotypes of dsRNA treatment

To verify the possible functions of the 20 *NIELOs*, RNAi was

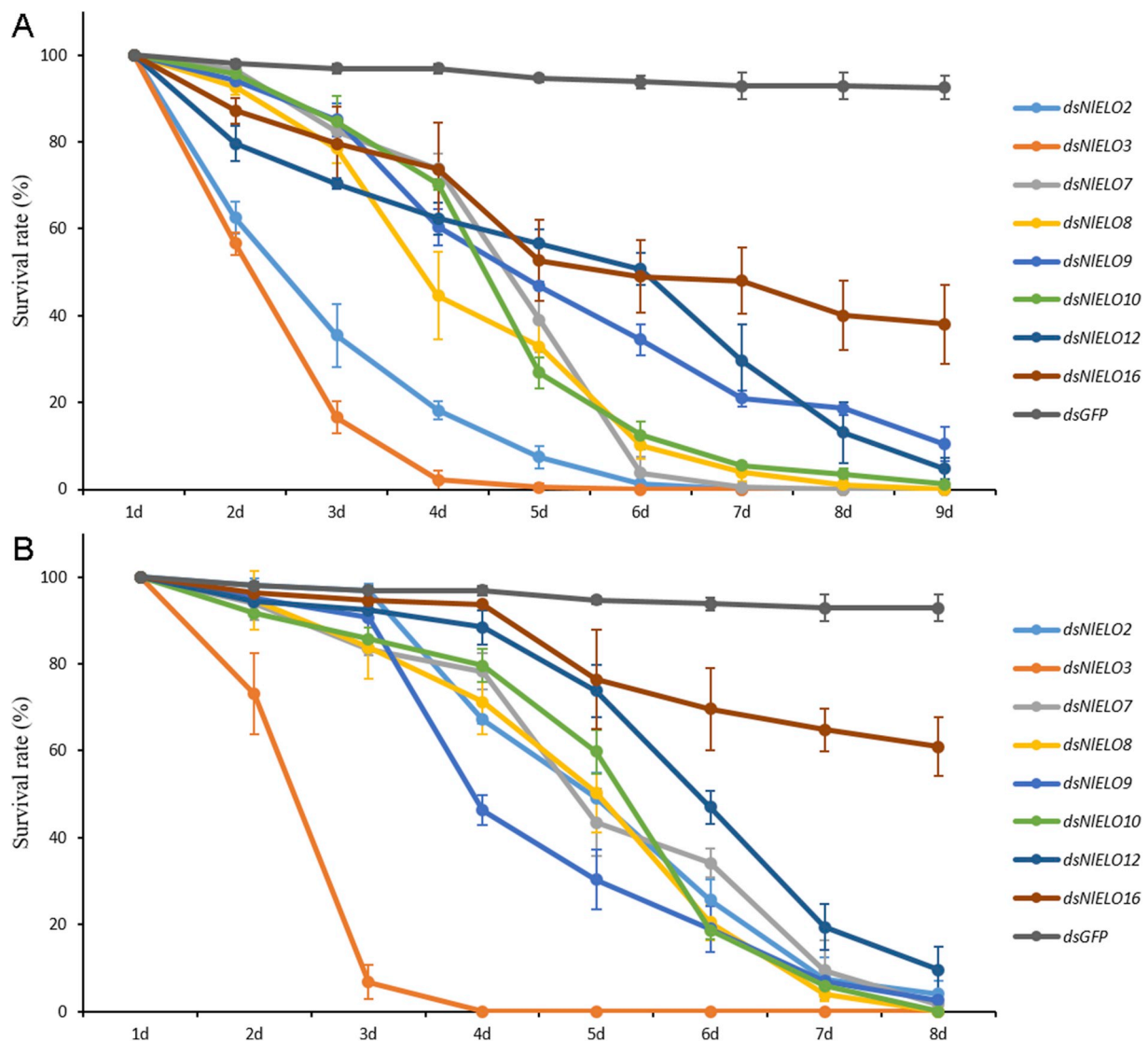


Fig. 4. Dynamic analysis of the survival rate following dsRNA injection. (A) dsRNA against *NIELO*s were injected at second-instar nymphs. dsGFP was injected as a negative control for the nonspecific effects of dsRNA; n = 100 insects. The values were calculated from three biological replicates (means \pm SEM). (B) dsRNA against *NIELO*s was injected at fourth-instar nymphs. dsGFP was injected as a negative control for the nonspecific effects of dsRNA; n = 100 insects. The values were calculated from three biological replicates (means \pm SEM).

conducted against each of these genes in the second instar (day 2, representing early instar nymphs), fourth instar (day 1, representing late-instar nymphs) nymphs, in male fifth instar (day 1, for testes and adults after emergence) nymphs and in 0–1 h male and female adults (for reproduction and embryos). To exclude off-target effects, RNAi experiments were replicated by choosing two non-overlapping regions as targets in fourth-instar nymphs. The results showed that no off-target effects occurred in the dsRNA injection experiments. RT-qPCR assays confirmed that all expressions of target genes were efficiently suppressed by dsRNA treatment (Fig. S3).

In general, the injection of two different regions of dsRNAs for one gene caused the same phenotype. RNAi against eight *NIELO*s (2, 3, 7, 8, 9, 10, 12 and 16) led to lethal phenotypes with high mortality in nymphs, indicating their essential roles during the normal development of *N. lugens* (Fig. 4). Intriguingly, the lethal phenotypes after injection of these 8 dsRNAs could be divided into two distinct classes: phenotype I, in which ds*NIELO*s 7, 9, 10 and 12-treated *N. lugens* died with a thin

body shape (Fig. 5); and phenotype II, in which ds*NIELO*s 2, 3, 8 and 16-treated *N. lugens* died with a liquid-covered body before or during ecdysis. In phenotype I, the whole bodies of treated *N. lugens* became very wizened and the size of the fat body was strongly reduced. Thus, the body weight as well as the triglyceride content of the dsRNA-treated *N. lugens* (fifth instar nymphs and female adults) showing lethal phenotype I were significantly decreased compared with the dsGFP-treated group of animals (Fig. 6). Furthermore, *N. lugens* treated with ds*NIELO10* had a second type of lethal phenotype when injected into fourth-instar (day 1) nymphs. Approximately 70% of treated *N. lugens* die in the process of eclosion. The remaining 30% of these *N. lugens* completed adult emergence, but were also malformed with small and abnormal forewings (Fig. 5D), and they finally died displaying phenotype I. Injection with ds*NIELO12* resulted in *N. lugens* with abnormal stylets after molting finished (Fig. 5C). This phenotype directly led to loss of the feeding ability, resulting in decreased food uptake and nutrition shortage consequently leading to phenotype I. Phenotype II dsRNA-

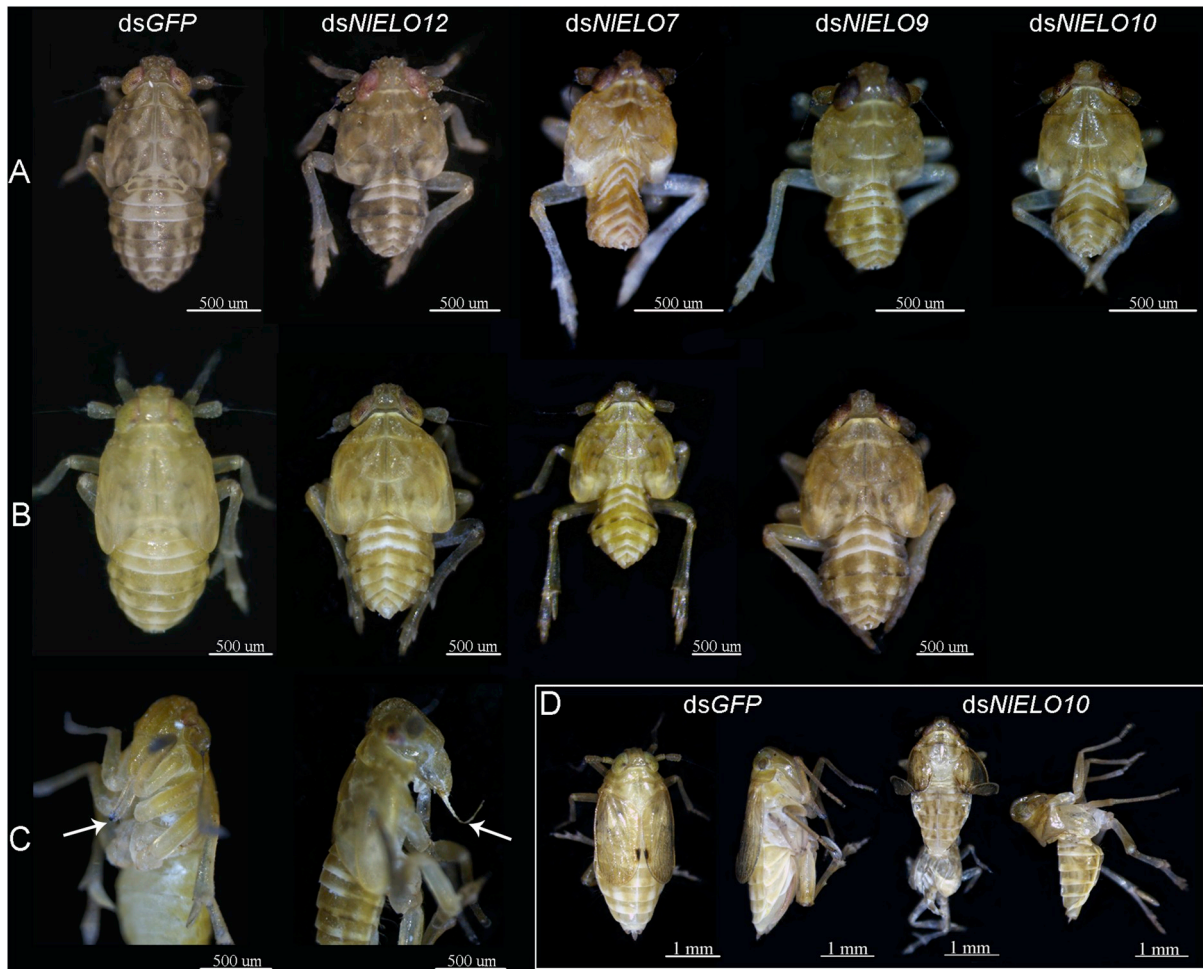


Fig. 5. Lethal phenotypes of *N. lugens* injected with dsRNA. dsRNAs treatments against *NIELOs* 7, 9, 10 and 12 at late stage second-instar (A) and early stage fourth-instar (B, C and D) nymphs. dsGFP was injected as a negative control for the nonspecific effects of dsRNA.

treated nymphs were covered by their own secreted honeydew (or water droplets) after molting, while dsGFP-treated nymphs could easily remove their secreted honeydew by gravity (Fig. 7). Interestingly, when the dsRNA-treated insects were cultured on horizontal tiled rice plants cushioned with filter paper, which helped to remove the insect-derived honeydew over time, the lethal effect of dsNIELOs 3 and 16-treated *N. lugens* was significantly obliterated with the emergence rate rising from almost 0% to 80.0% and 60.0% (Fig. S4), respectively. These results suggest that the dew-covered body surface was one of the main contributors to lethality and reveal the importance of the timely removal of honeydew during the *N. lugens* life cycle.

Next, the influences of *NIELO* silencing on insect cuticle were investigated by SEM observations. The results showed that almost all of the abdomens of dsGFP-treated *N. lugens* were covered with a hydrophobic layer, which may be vital for waterproofing. In contrast, almost no waxy coatings were found on the abdomens of the treated *N. lugens* (Fig. 7). Eoison Y-penetration showed that there was no obvious difference between dsNIELOs 2, 3, 8, 16- and dsGFP-treated *N. lugens* under physiological conditions (37 °C) (Fig. 7).

To test whether phenotype I (thin and wizen body shape) and phenotype II (deficiency of cuticular lipids) were associated with altered lipid contents, we analyzed the distribution and amounts of lipid reserves in the fat body of dsRNA treated nymphs. Nile-red staining was performed to visualize the lipid droplets. As shown in Fig. S5, the size of

visualized lipid droplets considerably decreased after *NIELOs* 2, 3, 7, 8, 9, 10, 12 and 16 knockdown, while *NIELOs* 7 and 9 injection resulted in an obvious reduction of lipid storage droplets in the fat body compared with the dsGFP-treated controls.

As many *NIELOs* were highly expressed in the testis and ovary, we conducted the RNAi experiments on the newly emerged adults to examine fertility. The average lifespan of adults, the average number of total eggs produced by one female adult and the average egg hatchability after RNAi were used to assess the roles of each ELO. The results showed that 5 ELO genes were indispensable in this experiment. The life expectancy of treated adults, the reproductive ability (total number of eggs) and the egg hatchability significantly decreased after knockdown of these five genes (*NIELOs* 1, 3, 7, 8 and 9) (Table 1). Notably, the reproductive ability and the egg hatchability were below 10 and 10% after knockdown of dsNIELOs 1 and 3. Upon dissection of the ovaries, no fully developed oocytes were observed on the fifth day after injection of dsNIELOs 1 and 3: the dysplastic oocytes stopped development and had wizened and cloudy shapes rather than the normal banana shapes (Fig. S6). Furthermore, egg hatchability was significantly decreased after knockdown of *NIELOs* 1, 3 and 7 in male adults suggesting their function in male fertility. It should be noted that among these 5 ELO genes essential for adult fecundity and embryogenesis, all but *NIELO1* were also indispensable for nymph development.

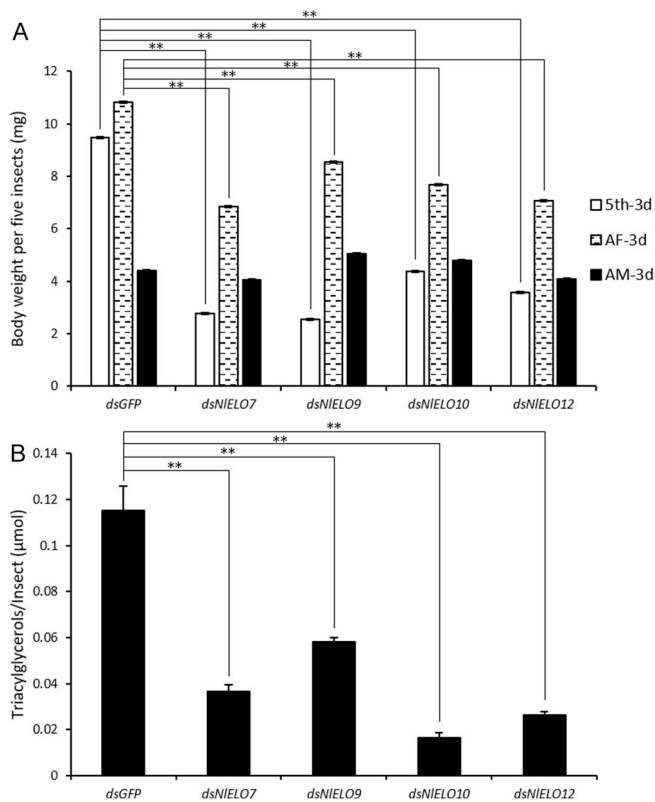


Fig. 6. Examination of body weight (A) and triglyceride content (B) in dsRNA-treated *N. lugens*. Body weight per five insects was examined in the RNAi treatments of the genes leading to phenotype I. The triglyceride content per insect was examined for RNAi treatments of the genes ($n = 10$). The *N. lugens* were treated with dsRNAs at the fourth and fifth instars. dsGFP was injected as a negative control. The values were calculated based on six biological replicates (mean \pm SD). ** $P < 0.01$ (Student's *t*-test), difference from dsGFP.

We also performed RNAi against the genes (*NIELOs* 4, 7, 10, 11, 12 and 18) that have high expression in the testis in male fifth-instar nymphs to observe the development of testes and adults after emergence, including lifespan of adults and the morphology of the testis. The emergence rates of ds*NIELOs* 10, 11, 12 and 18-treated nymphs significantly declined compared with the control (Table 1). The life expectancy of emerged adults significantly decreased after knockdown of *NIELOs* 4, 7, 10, 12 and 18. However, upon dissection, no abnormal testes were observed in the live adults (2 days after emergence).

3.4. Waterproofing and water retention assay

Experiments mimicking rain and desiccation were conducted to analyze whether water-proofing and water-retention of the insect cuticle were influenced when the expression of *NIELOs* 2, 3, 8 and 16 was suppressed. Experiments mimicking rain exposure showed that the survival rate of ds*NIELOs* 2, 3, 8 and 16-treated *N. lugens* declined significantly after 12 h compared to the control dsGFP-treated animals. Furthermore, ds*NIELO3*-treated *N. lugens* died within 36 h, ds*NIELOs* 2 and 16-treated *N. lugens* within 48 h, and ds*NIELO2*-treated *N. lugens* within 60 h, while dsGFP-treated *N. lugens* mostly survived during the observation period (Fig. 8A). In desiccation experiments, ds*NIELOs* 2, 3, 8 and 16-treated *N. lugens* were investigated under desiccation condition (< 5% RH). Treatments with *NIELOs* 2, 3 and 8-RNAi significantly increased susceptibility to desiccation. Survival time of ds*NIELOs* 2, 3 and 8-treated *N. lugens* significantly decreased by 79.2%, 43.3% and 56.0%, respectively, compared with the dsGFP control animals.

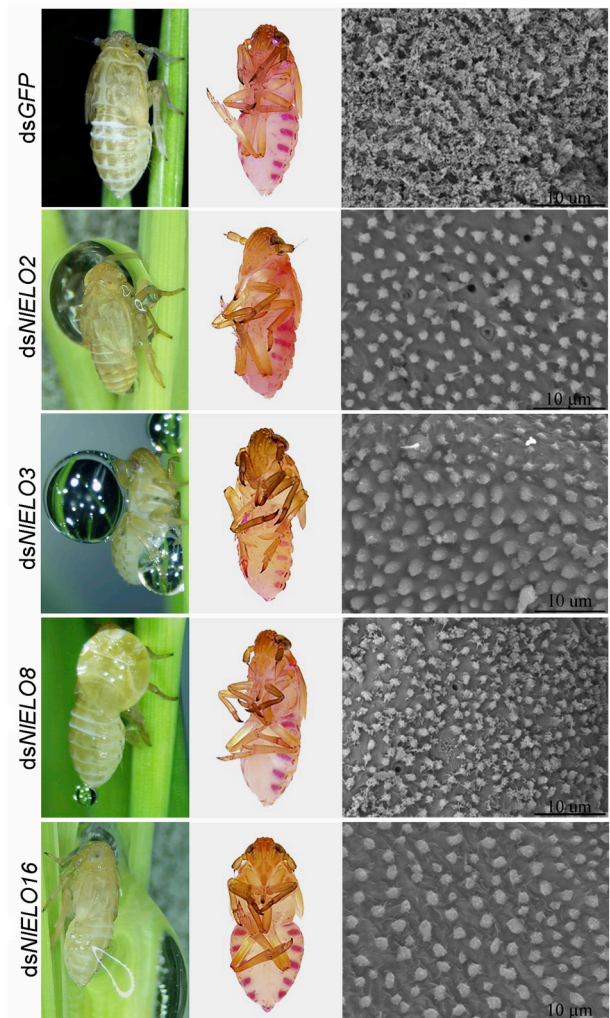


Fig. 7. Phenotypes of *N. lugens* injected with dsRNA. (Left) Effect of dsRNAs on the growth of third-instar nymphs. (Middle) Eosin Y penetration of dsRNA-treated fifth-instar nymphs (48 h). (Right) Scanning electron microscope analysis of the outermost layer. Fourth-instar nymphs (0–12 h) injected with dsRNAs were collected for SEM at the end of the fifth-instar nymph stage (48 h), while the insects were still alive. Images show parts of an abdominal venter from the fourth segment. dsGFP was injected as a negative control.

However, unexpectedly, the survival time increased significantly by 35.88% in the *NIELO16* silenced *N. lugens* (Fig. 8B). In the control treatment of 60–70% RH, there was no significant difference in the survival time of *N. lugens* between ds*NIELO16* and dsGFP treatment, but the survival time of ds*NIELOs* 2, 3 and 8-treated *N. lugens* still significantly decreased by 12.8%, 29.2% and 11.0%, respectively, when compared with the control.

3.5. Effect of *NIELO* knockdown on the level of CHCs

To further clarify the effects of *NIELOs* 2, 3, 8 and 16 RNAi knockdown on *N. lugens*, we investigated the CHC types and amounts in fifth-instar (3 d) nymphs treated with *NIELOs* 2, 3, 8, 16 and control dsRNA by GC-MS. Data from GC-MS confirmed that dsGFP-injected *N. lugens* had a mixture of different chain length *n*-alkanes and branched alkanes. ds*NIELO* treatments resulted in significant reductions in the CHC amounts in nymphs. There was no notable difference in the distribution and number of alkane peaks between the dsGFP-injected and

Table 1
Summary of phenotypes after RNAi for 20 ELO genes at four developmental stages in *N. lugens*.

Gene	dsRNA injection time and phenotypes				
	Second instar	Fourth instar	Fifth instar (♂) ^a	Male adult [*]	Female adult [*]
<i>NIELO1</i>	-	-	-	SLA, LEH	SLA, LEP [†] , LEH [†]
<i>NIELO2</i>	II [‡]	II [‡]	-	-	-
<i>NIELO3</i>	II [‡]	II [‡]	-	SLA, LEH	SLA, LEP [†] , LEH [†]
<i>NIELO4</i>	-	-	SLA	-	-
<i>NIELO5</i>	-	-	-	-	-
<i>NIELO6</i>	-	-	-	-	-
<i>NIELO7</i>	I [‡]	I [‡]	SLA	SLA, LEH	SLA, LEP, LEH
<i>NIELO8</i>	II [‡]	II [‡]	-	SLA	SLA, LEP, LEH [†]
<i>NIELO9</i>	I [‡]	I [‡]	-	SLA	SLA, LEP, LEH
<i>NIELO10</i>	I [‡]	I [‡]	LER, SLA	-	-
<i>NIELO11</i>	-	-	LER	-	-
<i>NIELO12</i>	I [‡] (A-st)	I [‡] (A-st)	LER, SLA	-	-
<i>NIELO13</i>	-	-	-	-	-
<i>NIELO14</i>	-	-	-	-	-
<i>NIELO15</i>	-	-	-	-	-
<i>NIELO16</i>	II [‡]	II [‡]	-	-	-
<i>NIELO17</i>	-	-	-	-	-
<i>NIELO18</i>	-	-	LER, SLA	-	-
<i>NIELO19</i>	-	-	-	-	-
<i>NIELO20</i>	-	-	-	-	-

The insects were treated as described in Materials and Methods. LEH, low egg hatchability; LEP, low egg production ability; LER, low emergence rate; SLA, short lifespan of injected adults; A-st, abnormal stylets.

^aRNAi against the ELO genes, which express high level in the testis.

^{*}The phenotypes listed were significantly decreased according to statistical test (Fig. S8 and Tables S4 and S5). Phenotypes I and II were classified as shown in Figs. 7, 8 and 10.

[†]Egg production ability or egg hatchability was below 10 or 10%, respectively.

[‡]The phenotypes were lethal.

-No obvious phenotypes.

those of treated nymphs, but the alkane amounts in ds*NIELOs* 2, 3 and 16-treated nymphs were significantly decreased compared with the control (Fig. 9A). The mean values of total alkanes per milligram of fresh body mass were 104.71 ± 14.62 ng/mg, 38.93 ± 5.43 ng/mg, 51.13 ± 3.78 ng/mg, 76.47 ± 9.51 ng/mg and 53.75 ± 5.26 ng/mg for ds*GFP*- and ds*NIELOs* 2, 3, 8 16-injected nymphs, respectively (Table S3). *N*-nonacosane (C₂₉) was the main CHC component, accounting for 40.63% of the total CHCs. It appears that the 62.8%, 51.2% and 48.7% reductions of total CHCs compared with the control in the *NIELOs* 2, 3 and 16 treatments, respectively, were due to reduction of different alkanes, mostly reduction of C₂₉ contents. In the ds*NIELO16*-treated group, the levels of C₁₄, C₁₆, C₁₇, C₁₈, C₁₉, C₂₀, C₂₂, C₂₆, C₂₇, C₂₈, C₂₉, C₃₀ and C₃₁ significantly decreased by 82.0%, 64.0%, 49.2%, 34.8%, 29.4%, 24.9%, 22.7%, 41.6%, 43.7%, 44.8%, 40.5%, 41.1% and 42.9%, respectively. However, only C₁₄, C₁₆, C₂₇, C₂₈, C₂₉ and C₃₁ levels in the ds*NIELOs* 2 and 3-treated groups significantly decreased by 34.0–88.6% and 34.6–91.8%, respectively. In contrast, although total CHCs in *NIELO8* decreased by 27.0%, the level of C₂₉ dramatically increased by 55.0% while predominantly branched alkanes were reduced compared with the control.

We next asked whether suppression of *NIELO* genes might perturb the expression of genes involved in lipid synthesis. For this purpose, we examined the expression profiles of two key genes coding for enzymes acting upstream of *NIELOs*, namely acetyl-CoA carboxylase (*NIACC*) and fatty acid synthase (*NIFAS*), in ds*NIELOs* 2, 3, 8 and 16-treated *N.*

lugens by qPCR. The results showed that knockdown of *NIELO2* significantly increased the transcript level of *NIACC*, while knockdown of *NIELO8* efficiently suppressed the transcript levels of *NIFAS*. The expressions of both *NIACC* and *NIFAS* were significantly suppressed in ds*NIELO16*-treated *N. lugens*. Finally, knockdown of *NIELO3* did not affect the expression levels of *NIACC* and *NIFAS* (Fig. 9B).

4. Discussion

Enzymes of the ELO family, which are required for the elongation of fatty acids to long-chain fatty acids, perform important biological functions in various organisms. Here, we identified and characterized 20 ELO genes of *N. lugens* based on assembled transcriptome and genome sequences and successfully performed RNAi against these genes observing specific phenotypes. RT-qPCR showed that these 20 ELO genes exhibited different temporal and spatial expression patterns, which underscored the complex relationship between the production of long chain lipids and developmental timing of different tissues. To the best of our knowledge, this is the first report on the comprehensive characterization and functional verification of the ELO gene family in an insect species. However, we need yet to understand how the ELOs coordinate their function with each other and with other enzymes in the CHC synthesis pathway (see below).

4.1. Some ELOs are essential, while some are dispensable for survival

While RNAi knockdown against 9 *NIELOs* (5, 6, 11, 13, 14, 15, 17, 19 or 20) did not lead to distinguishable phenotypes, we showed that 11 *NIELOs* (1, 2, 3, 4, 7, 8, 9, 10, 12, 16 and 18) were essential for survival. Based on the knock-down defects, we grouped the eight essential ELOs for nymphs into two phenotypic classes (phenotype I and II). Phenotype I *N. lugens*, caused by reduction of *NIELOs* 7, 9, 10 or 12, died with a thin and wizen body shape, and the body weight as well as the triglyceride content of the dsRNA-treated nymphs (5th, 3 day) and female adults (3 day) were significantly decreased compared with the ds*GFP*-treated group. Consistently, in these animals, the fat body was reduced suggesting that long chain fatty acids are needed for normal fat body morphology and function. *N. lugens* displaying phenotype II, through suppression of *NIELOs* 2, 3, 8 or 16, are characterized by a loss of cuticular barrier function inwardly and outwardly. The respective ELOs are conceivably involved in CHC production (see below).

There may be two reasons why we did not detect any visible dsRNA-induced phenotype for some ELOs. First, these ELOs may have redundant functions with other ELOs that compensate for their reduction. Alternatively, a subtle phenotype may have escaped our experimental readouts. In any case, further detailed studies including challenges with environmental hazards e.g. in penetration assays are needed to elucidate the function of these ELOs.

4.2. ELO function may not be conserved during insect evolution

In our comprehensive approach, we show that there are 20 ELO coding genes in *N. lugens* development and survival. The number of ELO coding genes varies considerably in insects ranging from 20 in the dipteran *D. melanogaster* to only 12 in the aphid *A. pisum*. Thus, ELO coding genes are fast evolving, and a one-to-one orthology seems improbable. Indeed, mutations may show severe defects in one insect species, while knockdown of its highest homologous gene in other insects does not cause similar phenotypes. For example, in the holometabolous insect *D. melanogaster*, *EloF* was reported to affect long-chain CHC biosynthesis and courtship behavior (Chertemps et al., 2007). By contrast, knockdown of the highest homologous gene to *EloF*, *NIELO15*, did not affect normal development of *N. lugens*, a hemimetabolous insect. Suppression of another *Drosophila* ELO gene, *noa*, caused severely

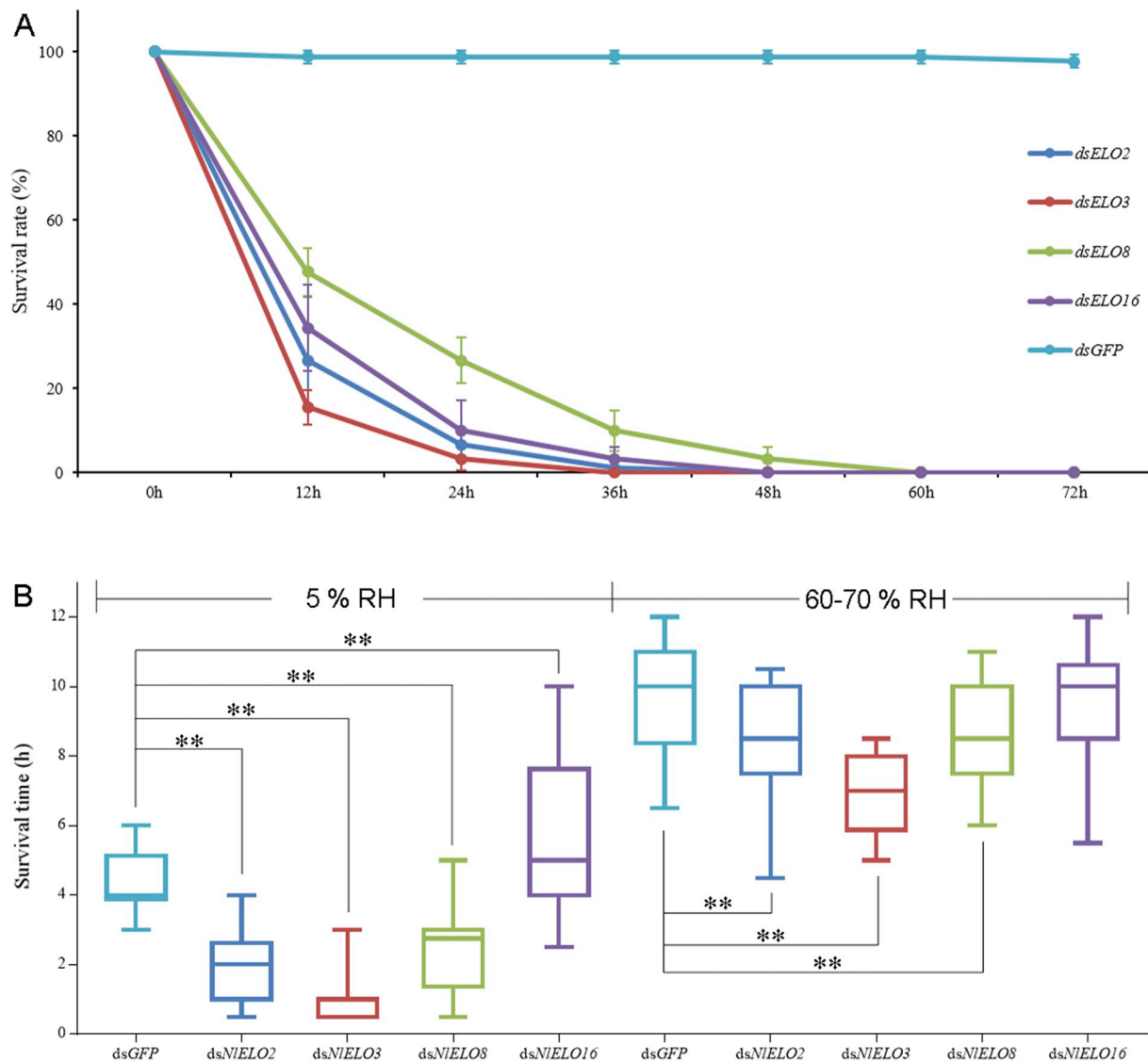


Fig. 8. Dynamic analysis of the survival rate and survival time following dsRNA injection. RNAi treatment of the genes leading to phenotype II was examined. (A) Effects of rain on the survival rate of fifth-instar nymphs three days post injection of dsNIELOs or dsGFP in fourth-instar nymphs; $n = 30$ insects. The values were calculated from three biological replicates (means \pm SEM). (B) Effect of desiccation on the survival time of fifth-instar nymphs three days post injection of dsNIELOs or dsGFP in fourth-instar nymphs; $n = 30$ insects. The values were calculated from three biological replicates (means \pm SEM).

reduced viability (Jung et al., 2007). However, silencing of its highest homologous gene, *NIELO20*, did not affect the normal development of *N. lugens*. Moreover, RNAi against any other *NLELO* did not cause similar phenotypes as did mutations in *EloF* and *noa*. We conclude that despite the high homology, the function of ELOs is not conserved at least between holo- and hemimetabolous insects.

4.3. Some ELOs are involved in CHC production and in desiccation resistance

ELOs, fatty acyl-CoA reductase and P450 decarbonylase participate in a common CHC biochemical pathway in insects. In the CHC synthesis pathway, ELOs are responsible for the addition of two carbon units to the carboxyl end of a fatty acid chain. Then a fatty acyl-CoA reductase converts long-chain fatty acids to fatty alcohols, which are subsequently oxidized to aldehydes and finally oxidatively decarbonylated to hydrocarbon by CYP4G enzymes (Chung and Carroll, 2015; MacLean et al., 2018; Qiu et al., 2012). In the present study, we mainly focused on *NIELOs*, which play vital roles in the production of cuticular lipids. Insect cuticular lipids are a complex cocktail of highly diverse CHCs,

sterols, fatty alcohols, triglycerides, wax esters, and other molecular species (Hadley, 1981). They form a hydrophobic coating to maintain water balance and to prevent desiccation and penetration of exogenous and potentially harmful substances (Gibbs, 2007). Generally, insect CHC profiles are species specific (Guillem et al., 2016). To a certain extent, the CHC profile of *N. lugens* is unique with sixteen compounds of saturated unbranched n-alkanes (C_{14} - C_{31}) and sixteen branched CHCs were detected on the cuticular surface. Our data are different from the CHC profiles previously reported in *Myrmica lobicornis* (C_{27} - C_{31}) (Guillem et al., 2016), *A. pisum* (C_{25} - C_{33}) (Chen et al., 2016) and *L. migratoria* (C_{25} - C_{33}) (Yu et al., 2016), but the high level of *n*-nonacosane (C_{29}) is as in *L. migratoria*.

It has been hypothesized that in order to adapt to changing humidity levels, the composition of the cuticle hydrophobic coat is adjusted dynamically to maintain water balance in insects in any situation (Chung and Carroll, 2015). In our study, dsRNA mediated suppression of *NIELOs* 2, 3, 8 and 16 expression in *N. lugens* resulted in reduction in CHCs and a smooth surface layer after molting, indicating that these four genes play important roles in CHC synthesis. It should be noted that the impact of dsNIELOs 2, 3, 8 and 16-treatment on CHC amounts

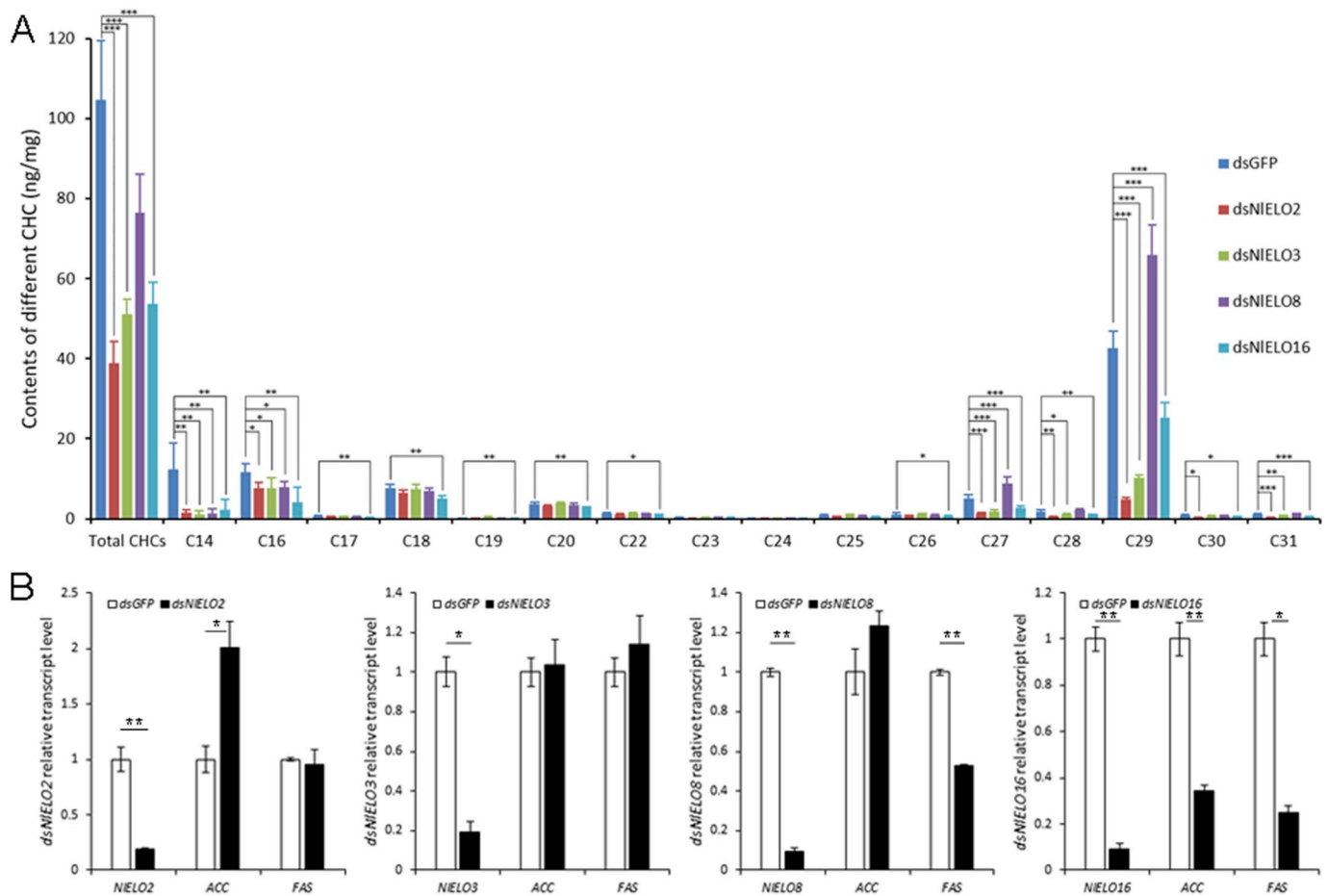


Fig. 9. (A) Effect of the CHC contents of *N. lugens* following dsRNA injection. The contents of total hydrocarbon and straight-chain alkanes of different lengths (C₁₄–C₃₁) were analyzed by GC-MS. The results were calculated from six biological replicates (nanograms per milligram of fresh body mass \pm SE). The asterisks *, ** and *** indicate significant differences at $P < 0.05$, $P < 0.01$ and $P < 0.001$, respectively, between dsNIELOs 2, 3, 8, 16- and dsGFP-treatments (Student's *t*-test). (B) ACC and FAS expression levels of dsRNA-treated *N. lugens* ($n = 8$ nymphs for fifth-instars). RT-qPCR and the $\Delta\Delta Ct$ method were used to analysis the relative expression levels of *ELO*, *ACC* and *FAS* genes. The relative expression levels of each gene were normalized using *NI18S* rRNA threshold cycle (Ct) values. The results of triplicate experiments are shown with the standard deviations.

varied. This may either rely on dsRNA-treatment efficiency or on the function of the respective ELO in producing fatty acids with a specific length.

In any case, our experiments to mimic rain exposure and immersion showed that *N. lugens* treated with dsNIELOs 2, 3, 8 and 16 were unable to survive on rainy days because they possibly lacked cuticle waterproofing. Furthermore, maintaining these insects on horizontal tiled rice plants cushioned with a filter paper that could help to remove the outermost water prevented lethality, suggesting that a dew-covered body surface was a main factor for the lethality and the importance of having a waterproof cuticular coat during *N. lugens* life cycle. Interestingly, barrier function against xenobiotics like Eosin Y is still retained in these animals suggesting that CHCs are mainly required for proofing against water but not larger molecules in *N. lugens*. In any case, the results of the desiccation experiments underlined that dsNIELOs 2, 3 and 8-treated *N. lugens* were sensitive to different levels of air humidity. By contrast, the survival time of dsNIELO16-treated *N. lugens*, which also lacked cuticular hydrophobicity, was much longer than that of dsGFP-treated animals under desiccation conditions. We speculate that silencing the expression of *NIELO16* disturbed not only CHC production, but also other, possibly physiological processes occurring in the fat body or any other organ, which are dependent on the product of *NIELO16*.

To date, a few insect ELO genes have been functionally analyzed and verified in *D. melanogaster*, namely *Bond* and *EloF* (Chertemps et al.,

2007; Ng et al., 2015). Although these two ELOs are involved in long-chain CHC synthesis, they have not yet been shown to be vital in the production of CHCs associated with cuticular waterproofing. Interestingly, however, contrary to the situation in dsNIELOs 2, 3, 8 and 16-treated *N. lugens*, in *eloF* mutant *D. melanogaster* adults the total amounts of CHCs was not reduced. Especially, C23 and C25 CHCs were increased at the expense of C27 and C29 CHCs in these animals. We propose two explanations for the naked surface of *N. lugens* with reduced *NIELOs* 2, 3, 8 or 16 activity. First, the function of these ELOs is needed in a positive feedback loop to induce the production of CHCs in general. As a consequence, the production of CHC ceases after knock-down of these *NIELOs*. We consider this as a less probable scenario. Second, long-chain CHCs produced by these ELOs are in theory needed for the attachment or adhesion of the CHC coat to the hydrophobic cuticle surface, the envelope, in *N. lugens* (Fig. 10).

Loss of surface CHCs is also observed when CHC quality is changed. The cytochrome P450 genes, *DmCYP4G1* of *D. melanogaster*, *LmCYP4G102* of *L. migratoria* and *CYP4G51* of *A. pisum* are responsible for the last step of CHC biosynthesis, the reductive decarboxylation of fatty aldehydes to the respective alkanes. RNAi against *LmCYP4G102* and *CYP4G51* caused a decrease in CHCs and an increase of mortality under desiccation condition (Chen et al., 2016; Yu et al., 2016). The cuticular waterproofing i.e. inward barrier efficiency in these cases remains to be investigated.

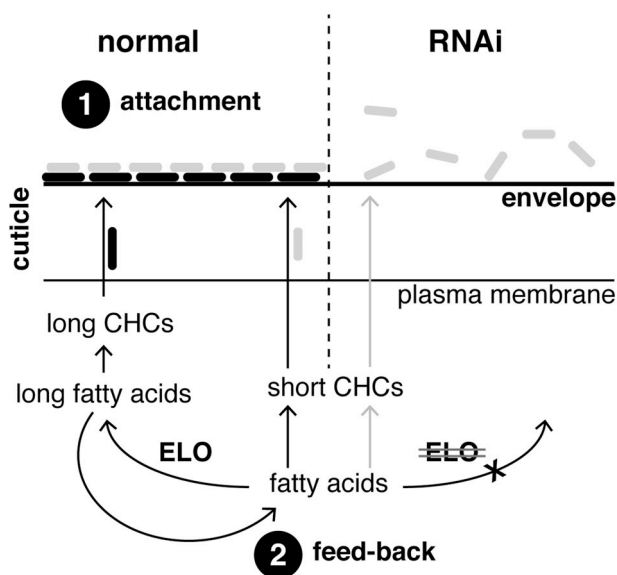


Fig. 10. Hypothetical model for the function of long-chain CHCs in establishing a hydrophobic coat on the cuticle surface of *N. lugens*. We propose that long-chain CHCs may possibly mediate attachment or adhesion of the CHC coat to the hydrophobic cuticle surface called the envelope. Alternatively, the products of ELOs may activate the production of CHCs in a positive feedback loop. In both cases, suppression of ELO function results in a depleted cuticular hydrophobic coat.

5. Conclusion

In summary, we identified 20 ELO genes in *N. lugens*. Four *NIELOs* (2, 3, 8 and 16) are essential for the production of CHCs, and seven *NIELOs* (1, 4, 7, 9, 10, 12 and 18) are important for the development and physiology of *N. lugens*. Our results reveal for the first time that ELOs function in the production of CHCs, which play vital roles in water repellency as well as water maintenance. These findings may serve as a basis for further biochemical studies on the substrate specificity of ELOs and the underlying molecular regulation mechanisms during development and survival of *N. lugens* without neglecting a possible impact of external i.e. ecological factors on ELO function.

Acknowledgements

This work was supported by the National Natural Science Foundation of China (31630057 and 31871954). BM was financed by the German Research Foundation in cooperation with the National Natural Science Foundation of China (grant number MO1714/10-1). We thank Dr. Yong-Liang Fan and Nan Chen for their kind help in CHC analysis.

Appendix A. Supplementary data

Supplementary data to this article can be found online at <https://doi.org/10.1016/j.ibmb.2019.03.005>.

References

Billeter, J.C., Atallah, J., Krupp, J.J., Millar, J.G., Levine, J.D., 2009. Specialized cells tag sexual and species identity in *Drosophila melanogaster*. *Nature* 461, 987–992.

Bottrell, D.G., Schoenly, K.G., 2012. Resurrecting the ghost of green revolutions past: the brown planthopper as a recurring threat to high-yielding rice production in tropical Asia. *J. Asia Pac. Entomol.* 15, 122–140.

Chen, N., Fan, Y.L., Bai, Y., Li, X.D., Zhang, Z.F., Liu, T.X., 2016. Cytochrome P450 gene, *CYP4G51*, modulates hydrocarbon production in the pea aphid, *Acyrtosiphon pisum*. *Insect Biochem Molec* 76, 84–94.

Chertemps, T., Dupontets, L., Labeur, C., Ueda, R., Takahashi, K., Saigo, K., Wicker-Thomas, C., 2007. A female-biased expressed elongase involved in long-chain hydrocarbon biosynthesis and courtship behavior in *Drosophila melanogaster*. *P Natl Acad Sci USA* 104, 4273–4278.

Chertemps, T., Dupontets, L., Labeur, C., Wicker-Thomas, C., 2005. A new elongase

selectively expressed in *Drosophila* male reproductive system (vol 333, pg 1066, 2005). *Biochem Biophys Res Commun* 336, 1002–1002.

Chung, H., Carroll, S.B., 2015. Wax, sex and the origin of species: dual roles of insect cuticular hydrocarbons in adaptation and mating. *Bioessays* 37, 822–830.

Denic, V., Weissman, J.S., 2007. A molecular caliper mechanism for determining very long-chain fatty acid length. *Cell* 130, 663–677.

Falcon, T., Ferreira-Caliman, M.J., Nunes, F.M.F., Tanaka, E.D., do Nascimento, F.S., Bitondi, M.M.G., 2014. Exoskeleton formation in *Apis mellifera*: cuticular hydrocarbons profiles and expression of desaturase and elongase genes during pupal and adult development. *Insect Biochem Molec* 50, 68–81.

Gibbs, A.G., 1998. Water-proofing properties of cuticular lipids. *Am. Zool.* 38, 471–482.

Gibbs, A.G., 2007. Waterproof cockroaches: the early work of J. A. Ramsay (Reprinted). *J. Exp. Biol.* 210, 921–922 (2007).

Guillem, R.M., Drijfhout, F.P., Martin, S.J., 2016. Species-specific cuticular hydrocarbon stability within European *Myrmica* ants. *J. Chem. Ecol.* 42, 1052–1062.

Guillou, H., Zadravec, D., Martin, P.G.P., Jacobsson, A., 2010. The key roles of elongases and desaturases in mammalian fatty acid metabolism: insights from transgenic mice. *Prog. Lipid Res.* 49, 186–199.

Hadley, N.F., 1981. Cuticular lipids of terrestrial plants and arthropods: a comparison of their structure, composition, and waterproofing function. *Biol. Rev.* 56, 23–47.

Huang, H.J., Xue, J., Zhuo, J.C., Cheng, R.L., Xu, H.J., Zhang, C.X., 2017. Comparative analysis of the transcriptional responses to low and high temperatures in three rice planthopper species. *Mol. Ecol.* 26, 2726–2737.

Jacobsson, A., Westerberg, R., Jacobsson, A., 2006. Fatty acid elongases in mammals: their regulation and roles in metabolism. *Prog. Lipid Res.* 45, 237–249.

Jung, A., Hollmann, M., Schafer, M.A., 2007. The fatty acid elongase NOA is necessary for viability and has a somatic role in *Drosophila* sperm development. *J. Cell Sci.* 120, 2924–2934.

Leonard, A.E., Pereira, S.L., Sprecher, H., Huang, Y.S., 2004. Elongation of long-chain fatty acids. *Prog. Lipid Res.* 43, 36–54.

Li, D.T., Chen, X., Wang, X.Q., Zhang, C.X., 2019. *FAR* gene enables the brown planthopper to walk and jump on water in paddy field. *Sci. China Life Sci.* 62. <https://doi.org/10.1007/s11427-018-9462-4>.

Livak, K.J., Schmittgen, T.D., 2001. Analysis of relative gene expression data using real-time quantitative PCR and the 2^{-ΔΔCt} method. *Methods* 25, 402–408.

Locke, M., 2001. The Wigglesworth Lecture: insects for studying fundamental problems in biology. *J. Insect Physiol.* 47, 495–507.

Lu, K., Zhang, X.Y., Chen, X., Li, Y., Li, W.R., Cheng, Y.B., Zhou, J.M., You, K.K., Zhou, Q., 2018. Adipokinetic hormone receptor mediates lipid mobilization to regulate starvation resistance in the brown planthopper, *Nilaparvata lugens*. *Front. Physiol.* 9.

MacLean, M., Nadeau, J., Gurnea, T., Tittiger, C., Blomquist, G.J., 2018. Mountain pine beetle (*Dendroctonus ponderosae*) CYP4Gs convert long and short chain alcohols and aldehydes to hydrocarbons. *Insect Biochem Molec* 102, 11–20.

Ng, W.C., Chin, J.S.R., Tan, K.J., Yew, J.Y., 2015. The fatty acid elongase Bond is essential for *Drosophila* sex pheromone synthesis and male fertility. *Nat. Commun.* 6.

Pan, P.L., Ye, Y.X., Lou, Y.H., Lu, J.B., Cheng, C., Shen, Y., Moussian, B., Zhang, C.X., 2018. A comprehensive omics analysis and functional survey of cuticular proteins in the brown planthopper. *P Natl Acad Sci USA* 115, 5175–5180.

Qiu, Y., Tittiger, C., Wicker-Thomas, C., Le Goff, G., Young, S., Wajnberg, E., Fricaux, T., Taquet, M., Blomquist, G.J., Feyereisen, R., 2012. An insect-specific P450 oxidative decarboxylase for cuticular hydrocarbon biosynthesis. *Proc. Natl. Acad. Sci. U. S. A.* 109, 14858–14863.

Szafer-Glusman, E., Giansanti, M.G., Nishihama, R., Bolival, B., Pringle, J., Gatti, M., Fuller, M.T., 2008. A role for very-long-chain fatty acids in furrow ingression during cytokinesis in *Drosophila* spermatocytes. *Curr. Biol.* 18, 1426–1431.

Tillman, J.A., Seybold, S.J., Jurenka, R.A., Blomquist, G.J., 1999. Insect pheromones: an overview of biosynthesis and endocrine regulation. *Insect Biochem Molec* 29, 481–514.

Tillmanwall, J.A., Vanderwel, D., Kuenzli, M.E., Reitz, R.C., Blomquist, G.J., 1992. Regulation of sex-pheromone biosynthesis in the housefly, *Musca domestica*: relative contribution of the elongation and reductive steps. *Arch. Biochem. Biophys.* 299, 92–99.

Tvrđik, P., Westerberg, R., Silve, S., Asadi, A., Jakobsson, A., Cannon, B., Loison, G., Jacobsson, A., 2000. Role of a new mammalian gene family in the biosynthesis of very long chain fatty acids and sphingolipids. *J. Cell Biol.* 149, 707–717.

Wang, Y.W., Yu, Z.T., Zhang, J.Z., Moussian, B., 2016. Regionalization of surface lipids in insects. *P Roy Soc B-Biol Sci* 283.

Wigglesworth, V.B., 1945. Transpiration through the cuticle of insects. *J. Exp. Biol.* 21, 97–113.

Xu, H.J., Xue, J., Lu, B., Zhang, X.C., Zhuo, J.C., He, S.F., Ma, X.F., Jiang, Y.Q., Fan, H.W., Xu, J.Y., Ye, Y.X., Pan, P.L., Li, Q., Bao, Y.Y., Nijhout, H.F., Zhang, C.X., 2015. Two insulin receptors determine alternative wing morphs in planthoppers. *Nature* 519, 464–467.

Xue, J., Zhou, X., Zhang, C.X., Yu, L.L., Fan, H.W., Wang, Z., Xu, H.J., Xi, Y., Zhu, Z.R., Zhou, W.W., Pan, P.L., Li, B.L., Colbourne, J.K., Noda, H., Suetsugu, Y., Kobayashi, T., Zheng, Y., Liu, S., Zhang, R., Liu, Y., Luo, Y.D., Fang, D.M., Chen, Y., Zhan, D.L., Lv, X.D., Cai, Y., Wang, Z.B., Huang, H.J., Cheng, R.L., Zhang, X.C., Lou, Y.H., Yu, B., Zhuo, J.C., Ye, Y.X., Zhang, W.Q., Shen, Z.C., Yang, H.M., Wang, J., Wang, J., Bao, Y.Y., Cheng, J.A., 2014. Genomes of the rice pest brown planthopper and its endosymbionts reveal complex complementary contributions for host adaptation. *Genome Biol.* 15.

Yu, Z.T., Zhang, X.Y., Wang, Y.W., Moussian, B., Zhu, K.Y., Li, S., Ma, E.B., Zhang, J.Z., 2016. *LmCYP4G102*: an oenocyte-specific cytochrome P450 gene required for cuticular waterproofing in the migratory locust, *Locusta migratoria*. *Sci Rep-Uk* 6.

Zheng, T.X., Li, H.S., Han, N., Wang, S.Y., Price, J.H., Wang, M.Z., Zhang, D.Y., 2017. Functional characterization of two elongases of very long-chain fatty acid from *Tenebrio molitor* L. (Coleoptera: Tenebrionidae). *Sci Rep-Uk* 7.

Zuo, W.D., Li, C.L., Luan, Y., Zhang, H., Tong, X.L., Han, M.J., Gao, R., Hu, H., Song, J.B., Dai, F.Y., Lu, C., 2018. Genome-wide identification and analysis of elongase of very long chain fatty acid genes in the silkworm, *Bombyx mori*. *Genome* 61, 167–176.